Clinical Neurophysiology 130 (2019) 469–473

Contents lists available at ScienceDirect

Clinical Neurophysiology

journal homepage: www.elsevier.com/locate/clinph

Subthalamic and pallidal oscillatory activity in patients with Neurodegeneration with Brain Iron Accumulation type I (NBIA-I)

Julius Huebl [a], Anahita Poshtiban [a], Christof Brücke [a], Sandy Siegert [a], Antje Bock [a], Henryk Koziara [b], Tomasz Kmiec [c], Rafał Rola [d,e], Tomasz Mandat [b], Andrea A. Kühn [a,f,g,*]

[a] Department of Neurology, Charité – Universitätsmedizin Berlin, Germany
[b] Departments of Neurosurgery, Institute of Psychiatry and Neurology, Warsaw, Poland
[c] Department of Neurology, Children's Memorial Health Institute, Warsaw, Poland
[d] First Department of Neurology, Institute of Psychiatry and Neurology, Warsaw, Poland
[e] Military Institute of Aviation Medicine, Department of Neurology, Warsaw, Poland
[f] NeuroCure, ExzellenzCluster, Charité – Universitätsmedizin Berlin, Germany
[g] Berlin School of Mind and Brain, Humboldt-Universität zu Berlin, Germany

ARTICLE INFO

Article history:
Accepted 23 December 2018
Available online 25 January 2019

Keywords:
Neurodegeneration with brain iron accumulation
Secondary dystonia
Deep brain stimulation
Local field potentials
Low frequency oscillations

HIGHLIGHTS

- Deep brain stimulation in the GPi and STN is effective in patients with secondary dystonia due to Neurodegeneration with Brain Iron Accumulation type I (NBIA-I).
- Basal ganglia low frequency activity is a prominent feature of hyperkinetic symptoms such as dystonia regardless of the etiology.
- Beta activity may reflect concurrent parkinsonism in dystonia-plus syndromes such as NBIA-I.

ABSTRACT

Objectives: Neurodegeneration with Brain Iron Accumulation type I (NBIA-I) is a rare hereditary neurodegenerative disorder with pallidal degeneration leading to disabling generalized dystonia and parkinsonism. Pallidal or subthalamic deep brain stimulation can partially alleviate motor symptoms. Disease-specific patterns of abnormally enhanced oscillatory neuronal activity recorded from the basal ganglia have been described in patients with movement disorders undergoing deep brain stimulation (DBS). Here we studied oscillatory activity recorded from the internal globus pallidus (GPi) and the subthalamic nucleus (STN) to characterize neuronal activity patterns in NBIA-I.
Methods: We recorded local field potentials (LFP) from DBS electrodes in 6 juvenile patients with NBIA-I who underwent functional neurosurgery. Four patients were implanted in the STN and two patients in the GPi. Recordings were performed during wakeful rest. An FFT-based approach was used to analyze the power spectrum in the target area.
Results: In all patients we found distinct peaks in the low frequency (7–12 Hz) and in 5 out 6 also in the beta frequency range (15–30 Hz) with the largest beta peak in the patient that presented with the most prominent bradykinesia. No distinct peaks occurred in the gamma frequency range (35–100 Hz). The oscillatory pattern did not differ between STN and GPi.
Conclusions: Here we show for the first time the oscillatory activity pattern in the STN and the GPi in juvenile patients with dystonia plus syndrome due to NBIA-I. The low frequency peak we found is in line with previous studies in patients with isolated idiopathic dystonia. In our cohort, the pallidal beta band activity may be related to more severe motor slowing in dystonia plus syndrome such as NBIA-I.
Significance: Our results further support the link between hyperkinetic motor symptoms such as dystonia and enhanced basal ganglia low frequency activity irrespective of the underlying etiology of dystonia.

* Corresponding author at: Charité – University Medicine Berlin, Department of Neurology, Augustenburger Platz 1, 13353 Berlin, Germany. Fax: +49 40 450 560 901.
E-mail address: andrea.kuehn@charite.de (A.A. Kühn).

https://doi.org/10.1016/j.clinph.2018.12.012
1388-2457/

1. Introduction

Neurodegeneration with brain iron accumulation (NBIA) comprises a group of hereditary disease entities that are characterized by progressive extra-pyramidal symptoms such as generalized dystonia and parkinsonism, but also cognitive decline and psychiatric symptoms are frequent. In about half of the patients with NBIA a mutation of the *PANK2*-gene is found. *PANK2* positive cases are classified as NBIA type I or panthotenate-kinase-associated neurodegeneration (PKAN) (Kurian and Hayflick, 2013). Typical radiologic findings include the eye-of-the-tiger-sign in the MR. The clinical course is variable but most often begins in early childhood with onset of limb dystonia. Treatment is mainly limited to supportive care and symptom control. Inspired by the success of deep brain stimulation (DBS) of the globus pallidus internus (GPi) as therapy for primary generalized dystonia (Vidailhet et al., 2005) this approach was recently applied in NBIA-I patients to aim at alleviation of dystonic symptoms (Timmermann et al., 2010). In this study an improvement of symptom severity of 29% was achieved after 2–5 months. Additionally, the subthalamic nucleus (STN) has been used successfully as a target for treatment of dystonia (Kleiner-Fisman et al., 2007). Only recently, a small sample of three patients with NBIA-I was treated with STN DBS and a moderate benefit was reported as measured by the Burke-F ahn-Marsden-Dystonia-Rating-Scale (BFMDRS) (Liu et al., 2017). However, despite this progress in therapy the underlying pathophysiology is only incompletely understood.

DBS gives the unique opportunity to study neuronal activity from the target area for electrode implantation. Studies in patients undergoing DBS for movement disorders have revealed disease-specific patterns of neuronal activity. This has led to a substantial progress in understanding the pathophysiology of movement disorders like Parkinson's disease (PD): here, elevated synchronization of beta oscillations has been shown to be related to bradykinesia and rigidity (Kühn et al., 2009). Complementary, enhanced low frequency activity was linked to hyperkinetic disorders like isolated dystonia and correlated with EMG activity in the dystonic muscles (Chen et al., 2006a). In summary the analysis of deep brain recordings in these patients have shaped the pathophysiological concept of movement disorders like PD and dystonia in a manner that these are now acknowledged as network disorders that can be modulated by DBS (Kühn and Volkmann, 2017).

In the present study, we therefore aimed to study the oscillatory activity in the STN and the GPi in patients with NBIA-I who underwent DBS for severe disabling dystonic symptoms. Because dystonia is a prominent feature in NBIA-I we expected enhanced synchronized activity in the low frequency range (Barow et al., 2014; Chen et al., 2006b; Neumann et al., 2012).

2. Patients and methods

We included 6 patients (mean age 16y ± 8.8, mean disease duration 8y ± 4) that presented with characteristic clinical and radiological features for NBIA-I who underwent implantation of DBS electrodes targeted at the STN (N = 4) or GPi (N = 2). Symptom severity was rated by trained movement disorder specialists (CB, TM) using the BFMDRS (see Table 1 for patient details). Patients were operated at the University hospital Warsaw (cases 1–5) and at Charité, University – Medicine Berlin (case#6), respectively. Quadripolar DBS electrodes (Medtronic, Minneapolis, MA, USA) model no. 3387 were implanted bilaterally in both GPi patients. Further details of surgery and electrode implantation for pallidal DBS have been described previously (Chen et al., 2006a). The intended target coordinates for contact 0 were 2–3 mm in front of the anterior commissure-posterior commissure (AC-PC) midpoint, 20–22 mm lateral to the midline of the third ventricle, and 4–6 mm below the AC-PC midpoint. In patients who received STN DBS the posterior-lateral portion of the STN was targeted with the model 3389 DBS electrode (Medtronic, Minneapolis, MA, USA). Here, the intended target coordinates were 12 mm lateral, 4 mm inferior and 3 mm posterior with reference to the AC-PC midpoint, corresponding to the sensorimotor area of the STN. Correct electrode placement was verified by post-operative imaging (CT cases 1–5 or MRI case 6) using the LEAD toolbox designed for DBS electrode localization (Horn and Kühn, 2015). However, more advanced and differentiated analysis of contact location was precluded because of low MRI quality as well as electrode and movement artifacts. In cases 3 and 5 postoperative CT scans were extraordinarily contaminated by movement artifacts. Here we had to manually co-register the preoperative MRI and postoperative CT scan (Figs. S3 and S4, cf. Supplementary Material for detailed description and imaging data). Electrode placement was further corroborated by effective stimulation as indexed by the amelioration in BFMDRS motor score (cf. Table 1). Patients or their caregivers provided informed consent for participation in the study and all measures were approved by the local ethics committees.

Electrode leads were externalized for 2 (range 1–3) days in order to allow for test stimulation before final implantation of the impulse generator. During this interval we recorded local field potentials (LFP) from the target area via the implanted DBS leads. Patients were at rest with eyes opened either lying supine in their beds or sitting in an arm chair. Recordings were started once a stable signal could be established that lasted for 5 minutes. Signals were recorded in a bipolar fashion from adjacent electrode contacts (0–1, 1–2, 2–3) with either a transportable EEG-system (Biopotential Analyzer Diana, St. Petersburg; cases 1–5, amplification 100,000 fold, sampling rate 1.5 kHz) or recorded with a stationary EEG-amplifier (Digitimer D360, Welfordshire, amplification 50,000) and sampled through an AD-converter (1401power, Cambridge Elecronic Design, CED, Cambridge, UK) at 1 kHz. Signals were recorded with Spike2-Software (Version 6.16, CED) and stored offline for subsequent analysis. We inspected the LFP traces and discarded epochs with artefacts (technical or due to patients' movements). Channels L2 (bipolar 1–2 left) and L3 (bipolar 2–3 left) of case#6 had to be excluded due to technical artifacts. In all cases we obtained 120 consecutive seconds of artefact free data for further analysis. The data was downsampled to a common sampling rate of 1 kHz. The spectral analysis was calculated using the Fast Fourier Transformation (FFT) function in Spike2 with a block size of 1024 and a Hanning window for each channel. This resulted in a frequency resolution of 0.98 Hz. Subsequent analyses were executed in MATLAB 7.14 (The MathWorks, Minneapolis, USA) and IBM SPSS Statistics V24.0 (IBM Corp., Armonk, New York, USA). We normalized the data by dividing each frequency bin by the standard deviation (SD) of the frequency range from 5 to 95 Hz to enable inter-individual and intra-individual comparison. After normalization we inspected each channel for occurrence of distinct peaks in the power spectrum. An elevation of spectral power qualified as a peak if at least three neighboring frequency bins showed substantially less power. The distribution of the peaks was assessed via the MATLAB histogram function (`hist`). The bin size corresponded to a frequency resolution of 1 Hz. Relative distribution of peaks at low frequency and beta band across the electrode was evaluated for the 4 patients with STN DBS. The maximum peak per hemisphere was set at 100% (i.e. the peak contact pair) in each patient and the relative power was calculated for the remaining contact pairs in each patient's hemisphere.

Table 1
Summary of clinical details.

Case	Age/gender	Medical centre	Predominant symptoms /genetics	Dystonia phenotype	Disease duration in years	Clinical scores pre OP	Clinical scores post OP	Medication at the time of surgery	DBS target	DBS parameters at 3 months postOP or later; monopolar stimulation
1	14/f	Warsaw	Hemidystonia dextra. c.573delC,c.1583C>T	Phasic	6	BFMDRS-M: 43 BFMDRS-D: 21 GDS: 8	BFMDRS-D-14 BFMDRS-M-19,5 GDS-3	Deferiprone	STN	**Left:**0–1-; 130 Hz; 90 μs; 1.5 V **Right:**0–1-; 130 Hz; 90 μs; 2.2 V
2	24/f	Warsaw	general.dyst.,oro-mandibular dyst., parkinsonism c.1561G>A p.G521R c.1583C>T p.T528M	Tonic	12	BFMDRS-M: 48 BFMDRS-D: 24 GDS: 7	BFMDRS-D-20 BFMDRS-M-40 GDS-5	Valproat, Clonazepam, Baclofen, Chlorpromazine	STN	**Left:**0–1-; 130 Hz; 90 μs; 1.2 V **Right:**0–1-; 130 Hz; 90 μs; 2.0 V
3	8/ m	Warsaw	Generalized dystonia c.573delC p.S191RfsX13 c.1561G>A,p.G521R	Tonic	7	BFMDRS-M: 70 BFMDRS-D: 30 GDS: 9	BFMDRS-D-27 BFMDRS-M-56 GDS-8	Deferiprone	GPi	**Left:**1–2-; 145 Hz; 90 μs; 3.2 V **Right:**1–2-; 145 Hz; 90 μs; 3.6 V
4	16/f	Warsaw	Focal dystonia- segmental dystonia, generalized dystonia. c.793G>A, c.1203delC	Phasic	8	BFMDRS-M: 68 BFMDRS-D: 26 GDS: 8	BFMDRS-D-22 BFMDRS-M-53 GDS-6	No medication	STN	**Left:**0–1-; 130 Hz; 90 μs; 1.4 V **Right:**0–1-; 130 Hz; 90 μs; 1.2 V
5	11/m	Warsaw	Oromandibular dystonia, generalized dystonia. c.1508C > G,c.1561G > A	Phasic	3	BFMDRS-M: 72 BFMDRS-D: 29 GDS: 9	BFMDRS-D-24 BFMDRS-M-56 GDS-6	No medication	STN	**Left:**0–1-;130 Hz; 90 μs; 4.2 V **Right:**0–1-;130 Hz; 90 μs; 3.6 V
6	25/m	Berlin	Oromandibular dystonia, generalized dystonia	Tonic	9	BFMDRS-M: N/A BFMDRS-D: N/A GDS: N/A	BFMDRS-D-21 BFMDRS-M-61.5 GDS: N/A	Clonazepam Procyclidine	GPi	**Left:**2-; 130 Hz; 90 μs; 3.3 V **Right:**2-; 130 Hz; 90 μs; 4.1 V

Burke-Fahn-Marsden Dystonia Rating **Disability** Scale (BFMDRS-D): 0–30.
Burke-Fahn-Marsden Dystonia Rating **Motor** Scale (BFMDRS-M): 0–120.
Global dystonia scale (GDS): 0–10.
STN: subthalamic nucleus.
GPi: Globus pallidus internus.

3. Results

Deep brain stimulation was effective in all patients leading to a mean post-operative improvement of 27.2 (±15.6) % in the BFMDRS motor ($p = 0.043$, Wilcoxon signed rank test, $N = 5$, pre-operative score of case#6 missing) and 18.5 (±8.6, $p = 0.002$) % in the BFMDRS disability score, respectively. In the 34 analyzed channels (6 patients × 6 channels, except 2 channels with technical artifacts of case#6) there were 24 peaks in the low frequency range that formed a narrow cluster from 7 to 12 Hz (Fig. 1). We also found 28 distinct peaks in the beta range (13–30 Hz) which occurred in all but one patient (case#4). Comparing the different target points there were no remarkable differences between STN and GPi in the distribution of low and beta frequency peaks (cf. Supplementary Material, Fig. S5). Low frequency and beta frequency peak activity was broadly distributed across the contact pairs in the whole patient group (Supplementary Fig. S5). When power was set to 100% at the peak contact pair within one hemisphere, relative power dropped on average to 69% (±19% SD) at the neighboring contacts pairs in the low frequency range and to 63% (±22% SD) in the beta frequency range. Wilcoxon signed rank tests for differences in relative power between contact pairs and between targets in the low and beta frequency band were all non-significant ($p > 0.05$, uncorrected, Supplementary Fig. S6).

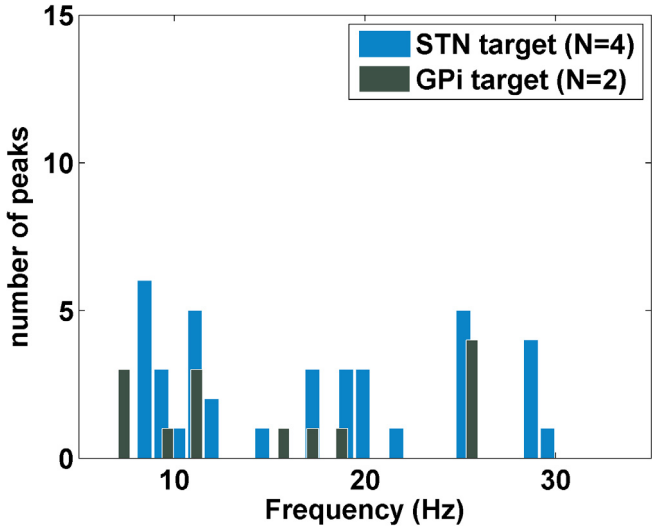

Fig. 1. The histogram shows the distribution of the peaks along the frequency range (x-axis). Blue bars reflect peaks in the STN (N = 4 patients), gray bars reflect peaks in the GPi (N = 2 patients). In the lower frequency range (5–12 Hz) there is less variability in frequency compared to the beta range (13–30 Hz). (For interpretation of the references to colour in this figure legend, the reader is referred to the web version of this article.)

The stimulation was delivered through contacts 0 and 1 in all 4 patients with STN DBS following a standard stimulation protocol. During follow-up visits stimulation parameter could be adjusted if no clinical effect had occurred. During initial test stimulation, however, the lower most contacts were most effective in all 4 STN patients furthermore underscoring a correct electrode placement. Using the same protocol, the two GPi patients showed a more effective stimulation after switching to contacts 1 and 2 and contact 2, respectively.

Interestingly, the largest beta peak occurred in case#2 (Fig. 2) who also had prominent bradykinesia alongside the generalized dystonia. She was bed ridden, unable to vocalize, to feed herself or to perform any daily activities (including hygiene). While the individual power spectra (Fig. 2) showed considerable variability of the peak frequency, especially in the beta range, there was no significant difference between the two targets STN and GPi as can be concluded from the widely overlapping 95% confidence intervals of both targets (see group data, Fig. 3).

4. Discussion

Here we showed for the first time the spectral power of resting activity in a group of six juvenile patients with NBIA-I, four of

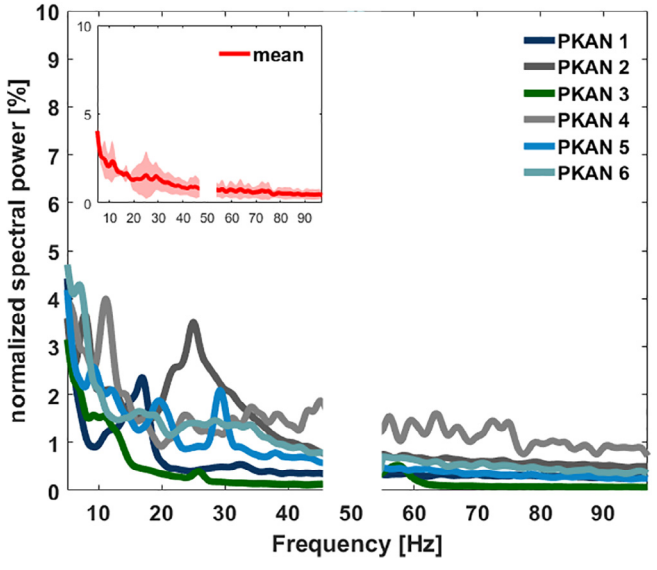

Fig. 2. The plots represent the average power spectrum of all LFP channels in each patient. Patients #3 and #6 were implanted in the GPi, all others were implanted in the STN. There are distinct peaks in the low frequency range (5–12 Hz) in all patients. In 5 out of 6 patients a second (or third) peak also occurred in the beta range (13–30 Hz). No peaks occurred in the gamma range (>30 Hz). The range of 50 Hz ±3 is excluded due to 50 Hz mains noise artefacts. The inset figure represents the group average with the 95% confidence interval.

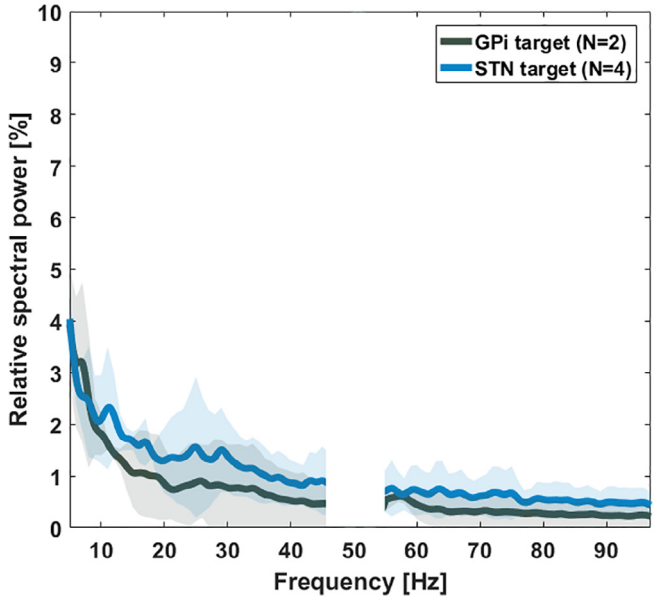

Fig. 3. The gray graph represents the average power spectrum of the patients with GPi DBS, the blue graph of the patients with STN DBS. The 95% confidence interval is indicated by the shaded blue and shaded gray area respectively. Note the variability in the beta range (20–30 Hz). The range of 50 Hz ±3 is excluded due to 50 Hz mains noise artefacts. (For interpretation of the references to colour in this figure legend, the reader is referred to the web version of this article.)

which had STN DBS and two had GPi DBS. Irrespective of the target region, we found distinct peaks in low frequency activity, which has been replicated as a signature of dystonic symptoms in the majority of the published studies (e.g. Barow et al., 2014; Chen et al., 2006b; Neumann et al., 2012). However, in a recent study comparing *intraoperative* LFP oscillations in the STN in a group of PD and primary dystonia patients beta peaks were also found in the dystonia group (Wang et al., 2016). In our NBIA-I sample the power spectrum also featured peaks in the beta range. Elevations in beta synchrony in the basal ganglia are regularly present during the dopamine deficient state in patients with PD (Hammond et al., 2007) and are associated with hypokinetic symptoms in these patients. It may thus be speculated that the peaks in the beta range in our NBIA-I patients may represent concurrent parkinsonism. In line with this hypothesis, patient 2 was severely affected and represented with severe bradykinesia along with most prominent beta band activity. On the other hand some patients received benzodiazepines which may induce beta peaks in the power spectrum as well (Blume, 2006).

Up to date intracranial recordings from patients with dystonia-plus syndromes are very rare. Whitmer and colleagues (Whitmer et al., 2013) studied 5 patients with dystonia syndromes (3 cases of secondary dystonia due to cerebral palsy (CP), 1 due to post encephalitis, 1 DYT-3+ Lubag dystonia). The patients with CP and Lubag dystonia showed peaks in the low frequency but also in the beta range. Another case series of two patients with myoclonus dystonia also reported elevated synchrony in the low frequency range without peaks at higher frequencies (Foncke et al., 2007). Recently, we could show that enhanced low frequency activity is also present in the thalamus and pallidum in patients with Tourette syndrome and correlates with severity in motor tics (Neumann et al., 2018). Together, these observations support the hypothesis that elevated low frequency activity is not specific to the disease entity but rather reflects a neurophysiological state marker for hyperkinetic symptoms. Future studies using implantable DBS sensing devices (Neumann et al., 2016) that allow long term recordings of neuronal activity from the DBS target regions may help to disentangle the functional role of elevated low and beta frequency activity by correlating clinical improvement with long term changes in neuronal activity pattern in these patients.

The moderate clinical effects of DBS in our patients are in line with previous reports of DBS in patients with NBIA-I. In the retrospective multi-center study of Timmermann et al. (2010) in which all patients received GPi DBS the mean improvement of symptom severity was 29% in BFMDRS. Similarly, Lumsden and colleagues (2013) reports small and inconsistent improvement in NBIA patients. A recent study with a small sample of three NBIA-I patients who received STN DBS, however, reports more relevant improvement of up to 73% (Liu et al., 2017). Due to the paucity of studies with DBS in NBIA-I patients there is not yet sufficient evidence to conclude whether STN or GPi DBS is superior. The limited sample size of our cohort neither enables this conclusion. However, following the hypothesis that elevated low frequency synchrony in the STN *and* the GPi reflects a pathologic network activity in the cortex-basal-ganglia loop our results support either target as a valid option to treat NBIA-I with DBS.

5. Conclusions

In summary our results strengthen the hypothesis that enhanced synchronization of low frequency activity in the basal ganglia is a pathophysiological signature of hyperkinetic movement disorders including isolated dystonia as well as dystonia-plus syndromes. Future studies will be required to determine if this activity is a suitable biomarker to tailor therapeutic measures such as closed loop DBS.

Conflict of interest

None of the authors have potential conflicts of interest to be disclosed.

Acknowledgment

Dr. G.-H. Schneider (Department of Neurosurgery, Charité – Berlin) performed surgery on case#6.

Appendix A. Supplementary material

Supplementary data to this article can be found online at https://doi.org/10.1016/j.clinph.2018.12.012.

References

Barow E, Neumann WJ, Brücke C, Huebl J, Horn A, Brown P, et al. Deep brain stimulation suppresses pallidal low frequency activity in patients with phasic dystonic movements. Brain 2014;137:3012–24.
Blume WT. Drug effects on EEG. J Clin Neurophysiol 2006;23(4):306–11.
Chen CC, Kühn AA, Hoffmann KT, Kupsch A, Schneider GH, Trottenberg T, et al. Oscillatory pallidal local field potential activity correlates with involuntary EMG in dystonia. Neurology 2006a;66(3):418–20.
Chen CC, Kühn AA, Trottenberg T, Kupsch A, Schneider GH, Brown P. Neuronal activity in globus pallidus interna can be synchronized to local field potential activity over 3–12 Hz in patients with dystonia. Exp Neurol 2006b;202(2):480–6.
Foncke EM, Bour LJ, Speelman JD, Koelman JH, Tijssen MA. Local field potentials and oscillatory activity of the internal globus pallidus in myoclonus-dystonia. Mov Disord 2007;22(3):369–76.
Hammond C, Bergman H, Brown P. Pathological synchronization in Parkinson's disease: networks, models and treatments. Trends Neurosci 2007;30(7):357–64.
Horn A, Kühn AA. Lead-DBS: a toolbox for deep brain stimulation electrode localizations and visualizations. Neuroimage 2015;107:127–35.
Kleiner-Fisman G, Liang GS, Moberg PJ, Ruocco AC, Hurtig HI, Baltuch GH, et al. Subthalamic nucleus deep brain stimulation for severe idiopathic dystonia: impact on severity, neuropsychological status, and quality of life. J Neurosurg 2007;107(1):29–36.
Kühn AA, Volkmann J. Innovations in deep brain stimulation methodology. Mov Disord 2017;32(1):11–9.
Kühn AA, Tsui A, Aziz T, Ray N, Brücke C, et al. Pathological synchronisation in the subthalamic nucleus of patients with Parkinson's disease relates to both bradykinesia and rigidity. Exp Neurol. 2009;215(2):380–7.
Kurian MA, Hayflick SJ. Pantothenate kinase-associated neurodegeneration (PKAN) and PLA2G6-associated neurodegeneration (PLAN): review of two major neurodegeneration with brain iron accumulation (NBIA) phenotypes. Int Rev Neurobiol 2013;110:49–71.
Liu Z, Liu Y, Yang Y, Wang L, Dou W, Guo J, et al. Subthalamic nuclei stimulation in patients with Pantothenate Kinase-Associated Neurodegeneration (PKAN). Neuromodulation 2017;20(5):484–91.
Lumsden DE, Kaminska M, Gimeno H, Tustin K, Baker L, Perides S, et al. Proportion of life lived with dystonia inversely correlates with response to pallidal deep brain stimulation in both primary and secondary childhood dystonia. Dev Med Child Neurol 2013;55(6):567–74.
Neumann WJ, Huebl J, Brücke C, Lofredi R, Horn A, Saryyeva A, et al. Pallidal and thalamic neural oscillatory patterns in tourette's syndrome. Ann Neurol 2018;84(4):505–14.
Neumann WJ, Huebl J, Brücke C, Ruiz MH, Kupsch A, Schneider GH, et al. Enhanced low-frequency oscillatory activity of the subthalamic nucleus in a patient with dystonia. Mov Disord 2012;27(8):1063–6.
Neumann WJ, Staub F, Horn A, Schanda J, Mueller J, Schneider GH, et al. Deep brain recordings using an implanted pulse generator in Parkinson's disease. Neuromodulation 2016;19(1):20–4.
Timmermann L, Pauls KA, Wieland K, Jech R, Kurlemann G, Sharma N, et al. Dystonia in neurodegeneration with brain iron accumulation: outcome of bilateral pallidal stimulation. Brain 2010;133:701–12.
Vidailhet M, Vercueil L, Houeto JL, Krystkowiak P, Benabid AL, Cornu P, et al. Bilateral deep-brain stimulation of the globus pallidus in primary generalized dystonia. N Engl J Med 2005;352(5):459–67.
Wang DD, de Hemptinne C, Miocinovic S, Qasim SE, Miller AM, Ostrem JL, et al. Subthalamic local field potentials in Parkinson's disease and isolated dystonia: An evaluation of potential biomarkers. Neurobiol Dis 2016;89:213–22.
Whitmer D, de Solages C, Hill BC, Yu H, Bronte-Stewart H. Resting beta hypersynchrony in secondary dystonia and its suppression during pallidal deep brain stimulation in DYT3+ Lubag dystonia. Neuromodulation 2013;16(3):200–5. discussion 205.